

# We are IntechOpen, the world's leading publisher of Open Access books Built by scientists, for scientists

6,900

Open access books available

186,000

International authors and editors

200M

Downloads

Our authors are among the

154

Countries delivered to

TOP 1%

most cited scientists

12.2%

Contributors from top 500 universities



WEB OF SCIENCE™

Selection of our books indexed in the Book Citation Index  
in Web of Science™ Core Collection (BKCI)

Interested in publishing with us?  
Contact [book.department@intechopen.com](mailto:book.department@intechopen.com)

Numbers displayed above are based on latest data collected.  
For more information visit [www.intechopen.com](http://www.intechopen.com)



# The Effect of Local Field Dispersion on the Spectral Characteristics of Nanosized Particles and their Composites

T.S. Perova<sup>1</sup>, I.I. Shaganov<sup>2</sup> and K. Berwick<sup>2</sup>

<sup>1</sup>Trinity College Dublin,

<sup>2</sup>Vavilov State Optical Institute, St.-Petersburg,

<sup>3</sup>Dublin Institute of Technology, Dublin

<sup>1,3</sup>Ireland

<sup>2</sup>Russia

## 1. Introduction

Infrared (IR) spectroscopy of micro- and nanosized particles and their composites is currently one of the most important enabling technologies in the development of micro- and nanostructures and their application to various areas of science and technology. Decreasing the characteristic size of metallic, dielectric and semiconductor materials results in a dramatic alteration to their optical, electrical and mechanical properties, allowing the fabrication of new materials with unique physical properties (Lamberti, 2008; Cao, 2004). These alterations in the optical properties are related to a quantum confinement effect, as well as to a dielectric, or electrostatic, confinement effect (Cahay et al., 2001; Chemla & Miller, 1986). The effect of quantum confinement is most pronounced in semiconductor materials, where the transition from the bulk state to the microcrystalline state causes a substantial change in the band structure and an enhancement of the non-linear electro-optical properties. Dielectric, or polarisation, confinement has a wider impact, since it influences the frequencies and intensities of absorption bands in the spectra of any condensed matter, including crystalline and amorphous solids, as well as liquids. This is because considerable changes in the polarisation of micro/nanoparticles occur, depending on their form and orientation with respect to the external electromagnetic field and the details of the spatial restriction.

So, the dielectric confinement effect is due to abrupt changes in the intensity of the internal ( $E_{in}(\nu)$ ), local electric field  $E_{loc}(\nu)$ , causing significant changes in the spectroscopic characteristics, depending on the direction of the external field  $E(\nu)$ , and the size and shape of the submicron sized particles, or micro-objects. Dielectric confinement occurs when the absorbing material consists of micro-particles with characteristic sizes significantly smaller than the wavelength of the probe beam. These particles are generally embedded in a transparent dielectric matrix, or deposited on a transparent substrate as an ultra-thin film (Fig. 1). A good analogy to these systems is that of an aerosol suspended in air or stained glass, that is, glass doped with small metal particles (Gehr & Boyd, 1996). In the long wavelength limit,  $d \ll \lambda$ , for the determination of the spectroscopic characteristics of micro-

particles with size  $d$  in the direction of dielectric confinement, one can use an effective medium theory model, while taking into account the dispersive local field (DLF) (Chemla & Miller, 1986; Schmitt-Rink, 1987; Cohen, 1973; Spanier & Herman, 2000). The important role of the local-field effect in the derivation of the equations of the effective medium theory of composites was considered in the paper by Aspnes, 1982.

The local-field approach is widely used for the analysis of the spectral characteristics of condensed matter under dielectric confinement. In particular, in Ref. (Liu, 1994), a description of the distribution of the  $p$ -component of the local electric field within the quantum wells in multi-quantum well GaAs-Al<sub>x</sub>Ga<sub>1-x</sub>As structures and the absorption band for intersubband transitions has been obtained, using a self-consistent integral equation for the local field. The development of the approach suggested for the analysis of the spectral features observed from materials based on porous structures is of particular importance (Spanier & Herman, 2000; Timoshenko et al., 2003; Golovan et al., 2007). These investigations largely involve extending the models used in effective medium theory.

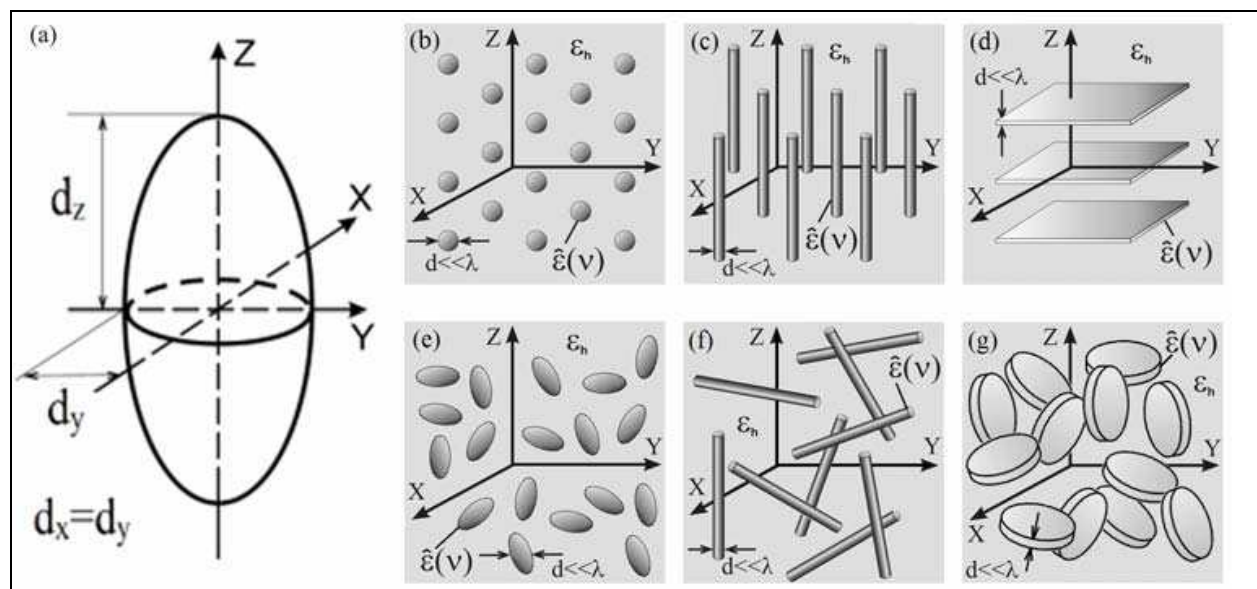


Fig. 1. a) The modeled spheroidal shape of the absorbing mesoparticles. Schematic depicting different types of size confinement for ordered (in (b) 3D confinement, c) 2D confinement ( $\vec{E} \perp z$ ) and d) 1D confinement ( $\vec{E} \parallel z$ ) and disordered (in (e) 3D confinement, f) 2D confinement and g) 1D confinement) mesoparticles

The effective medium theory (EMT) approach is widely used for modelling the optical and spectroscopic properties of a variety of composite media. The most extensively used EMT models are the Maxwell-Garnett (MG) and Bruggeman models, however other models are also used in some specific cases (Aspnes, 1982; Cohen et al., 1973; Spanier & Herman, 2000; Maxwell-Garnett, 1906; Bruggeman, 1935). For example in Ref. (Spanier & Herman, 2000), hybrid models, containing both phenomenological features and statistical theories of the dielectric function of dielectric media were used for modelling the infrared spectra from porous silicon carbide films. In Ref. (Mallet et al., 2005), an analysis of the accuracy of the modified Maxwell-Garnett equation, taking into account multiple scattering of light by the composite medium with spherical inclusions, has also been performed. In Ref. (Gehr & Boyd, 1996) the authors reviewed the theories and models developed for relating the linear

and non-linear optical properties of composite materials to those of the constituent materials, and to the morphology of the composite structure. The authors of Ref. (Hornyak et al., 1997) experimentally determined the size of gold nanoparticles, satisfying the quasi-static limit of applicability of the Maxwell-Garnett equation. As shown in this paper, inaccuracies in the MG expression, related to the scattering of light on large particles which do not satisfy the limit discussed earlier, can be eliminated by a dynamic modification of this expression (Foss et al., 1994). In the work (Ung et al., 2001), it was shown that the MG expression adequately describes the influence of inter-particle interactions on the position of the plasmon resonance band in colloidal solutions of gold. The influence of the local field on the enhancement of the light emission from various composite materials is described by (Dolgaleva et al., 2009).

In this Chapter, an overview of our recent work developing the effective medium approach and dispersive local field theory is presented. We also discuss the application of these models to nanocomposite materials, based on liquids and amorphous solids, for simulation of the experimentally obtained infrared spectra. We focus on a consideration of dielectric confinement only within the linear optical response. The influence of the dielectric confinement effect on the infrared absorption spectra of composite media will be demonstrated experimentally. We also present a theoretical analysis of this effect on the value of the frequency shift. The influence of the integrated intensity of the IR bands under consideration and the dielectric constant of the surrounding matrix will also be explored. The results obtained will assist in improving the reliability of IR spectral analysis.

## 2. Theoretical considerations

In the long-wave limit, when the absorbing material consists of micro-particles, with characteristic sizes significantly smaller than the wavelength of the probe beam, i.e. satisfying the condition  $d \ll \lambda$ , the spectroscopy of intermolecular interactions (IMI) can be used for analysis of their spectroscopic characteristics. The influence of the dielectric effect on the absorption spectra of molecular condensed systems was described for the first time in the work of Backshiev, Girin and Libov (BGL) (Backshiev et al., 1962; 1963), based on accounting for the spectral difference in the intensity of the effective, internal, field in the vicinity of the optical resonance and the average macroscopic field in condensed matter. A similar approach for calculating the spectral dependence of the microscopic susceptibility in the wavelength range of the intermolecular vibrations of organic liquids was used by Clifford & Crawford, 1966. In accordance with the BGL approach, the relationship between the micro- and macro-characteristics of condensed matter can be presented as

$$B(\nu) = \frac{2\pi \text{Im} \hat{\epsilon}(\nu) \theta(\nu)}{Nh} \quad (1a)$$

or

$$\frac{B(\nu)Nh}{2\pi} = \text{Im} \hat{\epsilon}(\nu) \theta(\nu) \quad (1b)$$

Here  $B(\nu)$  is the spectral density of the quantum intramolecular transition probability (Heitler, 1975),  $\text{Im} \hat{\epsilon}(\nu)$  is the imaginary part of the dielectric function in the vicinity of this transition and  $\theta(\nu) = |E_o(\nu) / E_{in}(\nu)|^2$  is the correction factor accounting for the spectral

difference between the internal, local, micro  $E_{in}(\nu)$  and the average macro  $E_0(\nu)$  fields of the electromagnetic wave in condensed matter. We note that the average electromagnetic field,  $E_0(\nu)$ , is considered here as a small perturbation and, therefore, the approach presented is still valid within the framework of linear molecular optics.

The  $B(\nu)$  spectrum in Eqn. (1) is considered to be characteristic of intramolecular quantum transitions with absorption. In case of the lattice vibrations, this spectrum is related to the dipole moment of the quantum transition, localized in a physically small volume of the crystal. The size of this elemental volume is significantly smaller than the wavelength of the probe beam, but is substantially larger than the size of the elemental crystal cell (Tolstykh et al., 1973). This conclusion can also be generalised to non-crystalline media. Indeed, it can be easily shown that expression (1b) corresponds to the spectrum of the imaginary part of the complex microscopic susceptibility of the medium  $\text{Im } \chi^{micro}(\nu) = \chi_2(\nu)$ , which, in accordance with the Lorentz local field model, is related to the macroscopic susceptibility of the isotropic medium by this expression

$$\hat{\chi}^{micro} = \frac{3\hat{\chi}}{\hat{\chi} + 3} \quad (2)$$

Where  $\hat{\chi}(\nu) = \chi_1(\nu) - i\chi_2(\nu)$  is the macroscopic dielectric susceptibility of the medium under consideration. Solving Eqn. (2) with respect to  $\text{Im } \chi^{micro}$  we obtain  $\chi_2^{micro} = \chi_2\theta(\nu)$ . Since  $\chi_2(\nu) = \text{Im } \hat{\epsilon}(\nu)$  we can consider  $\chi_2^{micro}(\nu)$  as the spectrum of  $\epsilon_2^{micro}(\nu)$ . This allows us to conclude that Eqn. (1a) corresponds to the spectral characteristics of a spherical micro-volume, or microparticle, of the condensed medium under consideration, with the particle size satisfying the condition  $\lambda \gg d \gg a_{molec}$  and represented by the following expression

$$\epsilon_2^{micro}(\nu) = \epsilon_2(\nu)\theta(\nu) \quad (3)$$

Using a continuum model of the local field allows us to use this expression with  $\theta(\nu) = 9 / |\epsilon(\nu) + 2|^2$  in order to establish the relationship between the dielectric loss spectrum of the bulk sample and that of the material under three dimensional (3D) size confinement, that is, for an isolated spherical particle. In general, the relationship between the local and average field in a condensed medium under 1D, 2D and 3D confinement can be written as (Ghiner & Surdotovich, 1994)

$$E_{in}(\nu) / E_0(\nu) = 1 + (\epsilon(\nu) - 1) / m, \quad (4)$$

where  $m = 1, 2$  and  $3$  respectively for the case of 1D, 2D and 3D confinement. The general equation describing the spectra of micro-objects,  $\epsilon_2^{micro}(\nu)$ , satisfying the conditions above can be expressed as

$$\epsilon_2^{micro}(\nu) = \epsilon_2(\nu)\theta(\nu) = \epsilon_2(\nu) |1 + (\epsilon(\nu) - 1) / m|^{-2} \quad (4a)$$

The use of molecular spectroscopy approaches when considering the spectral features characteristic of microparticles is justified. As shown by (Ghiner & Surdotovich, 1994), micro-particles, satisfying the conditions for dielectric confinement, can be considered as meso-oscillator molecules or meso-molecules, possessing their own spectroscopic

characteristic, i.e.  $\varepsilon_2^{micro}(\nu)$  (or  $\varepsilon_2^{meso}(\nu)$ ), spectrum. A similar conclusion follows from the work of (Chemla & Miller, 1986) where an expression similar to Eqn. (3) here was used to describe the spectral properties of semiconductor particles. It is worth noting that the basic mechanism responsible for the blue shift of the absorption spectra of nanoparticles with respect to their bulk counterpart is the decrease in the intermolecular interaction potential due to the reduction in, or elimination of, resonant dipole-dipole interactions of the molecules both inside and outside the particles. This decrease occurs as a result of the decrease in particle size from  $d \leq \lambda$  to  $d \ll \lambda$ , as well as the increase in the distance between the particles. The decrease in the resonant dipole-dipole interactions and, consequently, the intermolecular interaction potential can be taken into account by considering the dispersion of the effective field, from which the expressions (1a) and (4) are derived. We note that expression (4) describes only limited cases of dielectric confinement. In accordance with the expression for the local field inside a spherically shaped particle (Böttcher, 1952), the correction factor in Eqn. (4) can be written as

$$\varepsilon_2^{micro}(\nu) = \varepsilon_2(\nu)\theta(\nu) = \varepsilon_2(\nu) \left| 1 + L(\varepsilon(\nu) - 1) \right|^{-2} \quad (5)$$

$L$  is the form factor, the ratio of the semi-axes for an ellipsoidal particle shown in Fig. 1e. For an ellipsoid of revolution, the corresponding components of the form factor for two orientations of the electric field vector  $E$ , parallel,  $L_z$ , or perpendicular,  $L_{x,y}$ , to the rotation axis of the spheroid, are determined by the following expressions (Osborn, 1945; Golovan et al., 2003):

$$L_z = \frac{1}{1 - P^2} \left[ 1 - P \frac{\arcsin(\sqrt{1 - P^2})}{\sqrt{1 - P^2}} \right]; \quad L_{x,y} = \frac{1 - L_z}{2} \quad (6)$$

where  $P = d_z/d_x = d_z/d_y$  and  $d_z$  and  $d_x = d_y$  are the sizes of the corresponding polar and equatorial semi-axes of the spheroid (Fig. 1a). We note that for a spherical particle, the form-factor is  $L=1/3$  (Fig. 1b), while for a rod, along the short axis,  $L = 1/2$ , and along the long axis,  $L=0$  (Figs. 1c and 1f). For a strongly oblate spheroid stretched in the perpendicular direction,  $L=1$  (Figs. 1d and 1g).

Equation (5) shows that a particle with a dielectric function,  $\varepsilon$ , corresponding to the bulk material, can be considered as a particle with an effective microscopic spectrum  $\varepsilon_2^{micro}(\nu)$ . If this particle is embedded in a dielectric host matrix with  $\varepsilon_h > 1$ , then expression (5) can be written as

$$\varepsilon_2^{micro}(\nu) = \varepsilon_2(\nu)\theta(\nu) = \varepsilon_2(\nu)\varepsilon_h^2 \left| 1 + L(\varepsilon(\nu) - \varepsilon_h) \right|^{-2} \quad (7)$$

The dielectric loss spectrum for a diluted composite medium would be determined by spectrum  $\varepsilon_2^{micro}(\nu)$  and the volume concentration of particles  $f$  in the composite

$$\varepsilon_2^{comp}(\nu) = f\varepsilon_2(\nu)\theta(\nu) = f\varepsilon_2(\nu)\varepsilon_h^2 \left| 1 + L(\varepsilon(\nu) - \varepsilon_h) \right|^{-2} \quad (8)$$

Obviously, we ignore the resonant dipole-dipole interactions of the particles, which are practically insignificant when the filling factor,  $f$ , is smaller than 1%. This does not generate

significant errors in calculations until  $f$  is over 10%. Eqn. (8) was obtained earlier in paper (Shaganov et al., 2005). A more accurate equation can be obtained by modifying the Maxwell-Garnett expression using an effective media approach (Aspnes, 1982; Cohen et al., 1973; Spanier & Herman, 2000). For a composite medium containing absorbing particles of spheroidal shape, the corresponding expression can be written as

$$\frac{\hat{\varepsilon}_i(\nu) - \varepsilon_h}{L_i \hat{\varepsilon}_i(\nu) + (1 - L_i) \varepsilon_h} = \frac{f \cdot (\hat{\varepsilon}(\nu) - \varepsilon_h)}{L_i \hat{\varepsilon}(\nu) + (1 - L_i) \varepsilon_h} \quad (9)$$

where  $L_i$  is the corresponding component of the form factor,  $\hat{\varepsilon}_i(\nu)$  is the component of the tensor of the effective complex dielectric permittivity of the media and  $\hat{\varepsilon}(\nu)$  is the complex dielectric permittivity of the bulk material of the embedded particles. For  $L_i = 1/3$  expression (9) can be converted to the typical form of the Maxwell-Garnett equation.

$$\frac{\hat{\varepsilon}_i(\nu) - \varepsilon_h}{\hat{\varepsilon}_i(\nu) + 2\varepsilon_h} = \frac{f \cdot (\hat{\varepsilon}(\nu) - \varepsilon_h)}{\hat{\varepsilon}(\nu) + 2\varepsilon_h} \quad (10)$$

These expressions have been widely used in the past for modelling the spectral properties of metal-dielectric composites (Cohen et al., 1973; Foss et al. 1994; Hornyak et al., 1997; Ung et al., 2001). We note that the limits of applicability of this approximation are defined by the applicability of the electrostatic model of the effective medium, because this approximation does not take into account the size of the particles under consideration. A more precise approach is required to consider so-called dynamic polarisation, which takes into consideration the size of the particle, and its interaction time, with the field of the electromagnetic wave (Golovan et al., 2003; 2007). It is reasonable to assume that dynamic polarisation is significant only in the visible range, playing a minor role in the mid-infrared range, to a first approximation. Solving expression (9) for the desired value, we obtain the following expression for the dielectric permittivity spectrum of the composite media

$$\hat{\varepsilon}_i = \frac{f(\hat{\varepsilon}(\nu) - \varepsilon_h) \varepsilon_h (1 - L_i) + \varepsilon_h [L_i \hat{\varepsilon}(\nu) + (1 - L_i) \varepsilon_h]}{L_i \hat{\varepsilon}(\nu) + (1 - L_i) \varepsilon_h - f \cdot (\hat{\varepsilon}(\nu) - \varepsilon_h) L_i} \quad (11)$$

From expression (10), the effective dielectric loss spectrum of the ordered composite medium,  $\text{Im}(\hat{\varepsilon}_i(\nu))$ , in general, can be presented in the following form.

$$\text{Im}(\hat{\varepsilon}_i(\nu)) = \frac{A_2 B_1 - A_1 B_2}{B_1^2 + B_2^2} \quad (11a)$$

where

$$A_1(\nu) = \{(1-f)(1-L_i)\varepsilon_h + [f(1-L_i) + L_i]\varepsilon_1(\nu)\}\varepsilon_h$$

$$A_2(\nu) = [f(1-L_i) + L_i]\varepsilon_h \varepsilon_2(\nu)$$

$$B_1(\nu) = (1-L_i)\varepsilon_h + f\varepsilon_h L_i + L_i(1-f)\varepsilon_1(\nu)$$

$$B_2(\nu) = L_i(1-f)\varepsilon_2(\nu)$$

Here  $\varepsilon_1(\nu)$  and  $\varepsilon_2(\nu)$  are the real and imaginary parts of the dielectric permittivity spectrum of the particle material in the bulk state  $\hat{\varepsilon}(\nu) = \varepsilon_1(\nu) - i\varepsilon_2(\nu)$ . For a random particle orientation, the effective dielectric loss spectrum of the isotropic composite medium can be presented as

$$\varepsilon_2^{eff}(\nu) = \frac{1}{3} \sum_{L_i} \varepsilon_{2i}(\nu) \tag{12}$$

where the addition of the index  $L_i$  takes into account the difference in form factor of the particles in the  $x, y, z$  directions. For the specific case of 1D, 2D and 3D confinement, and at  $f \ll 1$ , Eqn.(11) can be transformed to the more simple form given in Ref. (Shaganov et al., 2010)

$$\text{Im}(\hat{\varepsilon}_i(\nu)) = f \varepsilon_2(\nu) \theta_{iD}(\nu) \tag{13}$$

where  $\theta_{iD}(\nu)$  is the correction factor for the internal, local, field, acting on the particles under 1D, 2D and 3D dielectric confinement, in agreement with Expression (4) obtained previously (Shaganov et al., 2005).

$$\theta_{iD}(\nu) = \left( 1 + \frac{\hat{\varepsilon}(\nu) - \varepsilon_h}{m_i \varepsilon_h} \right)^{-2} \tag{14}$$

where  $i = m_i = 1, 2, 3$  for 1D, 2D and 3D confinement, respectively. For randomly oriented particles, expressions (13) and (14) can be transformed to the following form (Shaganov et al., 2010)

$$\varepsilon_2^{eff}(\nu) = \frac{1}{3} f \varepsilon_2(\nu) \left[ 3 - m_i + m_i^3 \varepsilon_h^2 \cdot |\hat{\varepsilon}(\nu) + (m_i - 1)\varepsilon_h|^{-2} \right] \tag{15}$$

It is worth noting that the expressions above are valid only for diluted composites, where the resonant dipole-dipole interaction between the particles can be neglected. Depending on the intensity of the absorption band, or oscillator strength, resonant interactions between the particles become significant when the volume fraction of the particles is in the range  $f = 0.1 - 0.2$ . In this case, the local field factor,  $\theta_{iD}(\nu)$ , becomes dependent on the particle concentration (Shaganov et al., 2005) and expression (15) is transformed to the following (Shaganov et al., 2010)

$$\varepsilon_2^{eff}(\nu) = \frac{1}{3} f \varepsilon_2(\nu) \left[ 3 - m_i + m_i^3 \varepsilon_h^2 \cdot |(\hat{\varepsilon}(\nu) - \varepsilon_h)(1 - f) + m_i \varepsilon_h|^{-2} \right] \tag{15a}$$

We note that Eqn. (15a) can be used not only in the limited cases of 1D, 2D and 3D confinement, but also for composites of spheroidal particles where the ratio of the semi-axes  $P \geq 10$  or  $P \leq 0.1$ . For intermediate values of  $P$ :  $0.2 < P < 9$ , account must be taken of the specific values of the form factors for the three axes of the spheroidal particles, assuming that  $m_i = 1/L_i$  (see Shaganov et al., 2010 for details).

As shown in Ref. (Shaganov et al., 2005), the difference between the spectral characteristics of the bulk materials and those from a composite of micro-particles can be substantial. The shift in the peak position of the intense absorption bands due to dielectric confinement can be far greater than the linewidth of the absorption band observed in the bulk material. The peak position, or maximum frequency, for isolated particles in the case of 3D confinement ( $\nu_{3D}$ ) is close to Fröhlich's frequency ( $\nu_F$ ) (Fröhlich, 1949), corresponding to the condition  $\varepsilon_1(\nu_F) = -2\varepsilon_h$ . The maximum shift in the peak position of the absorption spectrum occurs for 1D confinement, where the peak position is observed at a frequency  $\nu_l$ , satisfying the minimum of the function  $\varepsilon_1(\nu_l) = 0$ . Thus, it is not surprising that the values for  $\nu_l$ , obtained

from calculations for polar crystals, coincide with the frequency of the corresponding band of longitudinal optical (LO) phonon vibrations. The absorption spectra of the amorphous media at frequencies  $\nu_l$  has already been discussed in numerous papers (Berreman, 1963; Röseler, 2005; Tolstoy et al., 2003; Iglesias et al., 1990; DeLeeuw & Thorpe, 1985). Conclusions on the size dependent nature of this effect have been made earlier in the theoretical work of (Lehmann, 1988). We would like to emphasise that we obviously cannot discuss LO-phonons in amorphous solids and, in particular, in liquids, since the new bands observed arise as a result of the interaction of the transverse electromagnetic wave with a condensed medium under dielectric confinement, when the contribution from surface vibrations becomes greater than that from the bulk. The maximum frequency of the spectrum from a composite medium, for 2D confinement, lies between the frequencies for 1D and 3D dielectric confinement, i.e.  $\nu_{3D} < \nu_{2D} < \nu_{1D}$ . In practice, the microparticles will not all be spheroidal, particularly in microcrystalline powders, for which the shape of particles often depends on the crystalline structure of the material. For a more detailed discussion see Shaganov et al., 2010.

### 3. Results and discussion

The objective of this section is to demonstrate, both theoretically and experimentally, the role of various types of dielectric confinement on the absorption spectra of organic liquids and amorphous solids. Amorphous SiO<sub>2</sub> and three organic liquids of spectroscopic grade viz. benzene (C<sub>6</sub>H<sub>6</sub>), chloroform (CHCl<sub>3</sub>), and carbon disulphide (CS<sub>2</sub>), have been chosen for the experiments, because of their well characterized, strong absorption in the infrared range (Zolotarev et al., 1984; Barnes & Schatz, 1963).

#### 3.1 Calculations

The method in which dielectric mesoparticles are embedded in the host medium is important in the engineering of the optical properties of a composite. For example, depending on the alignment and distribution of the mesoparticles in the host medium, the composite medium can possess optical anisotropy, which is apparent in phenomena such as birefringence, anisotropy in the real part of the refractive index, and dichroism, anisotropy in the imaginary part of the refractive index (Golovan et al., 2007). In this study, we discuss the influence of dielectric confinement on the resonant part of the dielectric permittivity, leading to phenomena such as a spectral shift in the resonant absorption band and its anisotropy. We consider two extreme cases only, viz. completely ordered and completely disordered (randomly oriented) dielectric mesoparticles, uniformly distributed in a host medium (Fig. 1). It is worth noting that deliberately varying the degree of mesoparticle disorder in a composite medium can be used in order to tune its optical properties. Eqns. (8), (11a) and (12), (15) describe dielectric loss spectra for completely ordered and disordered composites, respectively. Note that in the case of a disordered composite, as described by Eqn. (12), (15) and (15a), the solution consists of two bands for all mesoparticles, with the exception of those with a spherical shape. The splitting apparent in the dielectric loss spectrum and, therefore, in the absorption spectrum of the composite, is most pronounced for 1D confinement.

In the calculations presented in Figs. 2-4, and summarized in Tables 1 and 2, we used Eqns. (11a) and (12) for 1D, 2D and 3D confinement. These situations can also be described using the simplified Eqns. (8) and (15a). In Table 1, experimental data described in Section 3.2 are also shown for comparison. Calculations have been performed for liquid benzene, chloroform and carbon disulphide at  $f = 0.1$  (for  $\epsilon_h = 11.56$  (Si) and  $\epsilon_h = 13.6$ ) and additionally for carbon

disulphide at  $f = 0.1$  and  $\epsilon_h = 3$ , and for benzene at  $f = 0.1$  and  $\epsilon_h = 2.2$ ,  $\epsilon_h = 5$ , and  $\epsilon_h = 16$  (Ge). The optical constants in the infrared range for benzene, chloroform and carbon disulphide were taken from references (Zolotarev et al., 1984; Barnes & Schatz, 1963). The value of  $\epsilon_h = 13.6$  was an average, calculated by taking the square root of the product of  $\epsilon_{Si} = 11.56$  and  $\epsilon_{Ge} = 16$ . This allowed us to model liquids films between a Ge ATR prism and a Si slide in a GATR attachment as described in the experimental Section. Additional calculations for carbon disulphide at  $\epsilon_h = 3$  and for benzene at  $\epsilon_h = 2.2$  were performed to illustrate absorption band splitting in a disordered composite, apparent on the bottom panels of Fig.2 (c and d).

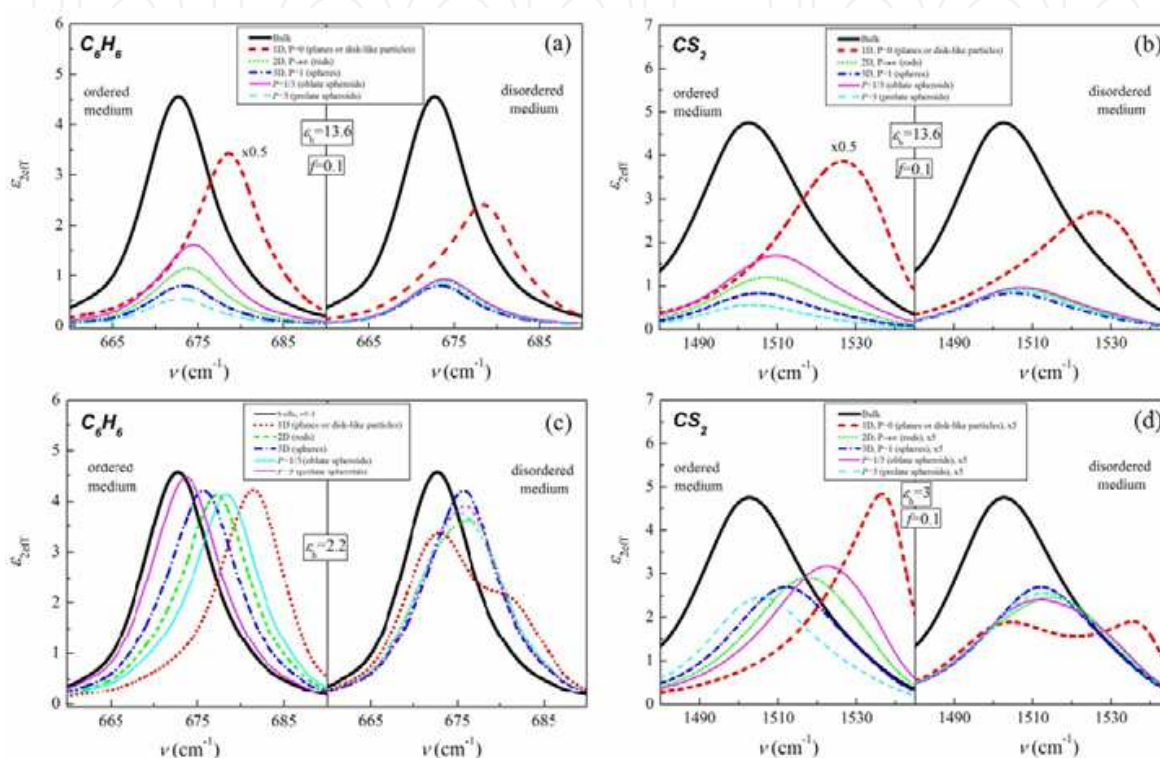


Fig. 2. Dielectric loss spectra calculated for ordered and disordered mesoparticles with filling factor  $f=0.1$  under different confinement conditions for (a) benzene and (b) carbon disulphide in host media with  $\epsilon_h=13.6$  (Si/Ge) and for (c) benzene at  $\epsilon_h=2.2$  and (d) carbon disulphide at  $\epsilon_h=3$

As can be seen from Fig. 2, by changing the particle shape for ordered mesoparticles, we can gradually change the peak position of the absorption spectrum of the composite media in the range of  $15 \text{ cm}^{-1}$  for benzene and  $30 \text{ cm}^{-1}$  for  $\text{CS}_2$ . The peak position of the dielectric loss spectrum for oblate spheroids ( $P = 1/3$ ) is close to the peak position corresponding to 1D confinement in planes or disks (Figs. 1d and 1g), while the peak position for prolate spheroids ( $P = 3$ ) is close to that observed from bulk benzene and carbon disulphide, since the amount of dielectric confinement is reduced in the direction of the field, that is, along the rotation axis of the particles.

The situation for disordered mesoparticles is quite different. In both cases, namely  $P = 1/3$  and  $P = 3$ , the dielectric loss spectra are close to the spectrum from spherical particles. It is interesting that, in this case, the dielectric loss spectrum from oblate spheroids is closer to the spectrum of the bulk, while the spectrum for prolate spheroids is closer to the spectrum characteristic of 1D confinement. The similarity of the dielectric loss spectra for  $P = 1/3$  and  $P = 3$  to the spectrum from spherical particles under 3D confinement can be explained as

being due to averaging of the disordered spheroids in every direction, resulting in an isotropic medium, the properties of which will be close to those in spherical particles. This is true despite the strong anisotropy of the particles themselves. From a comparison of Figs. 2(a) and 2(c) for  $C_6H_6$  and Figs. 2(b) and 2(d) for  $CS_2$  it can also be seen that splitting of the dielectric loss spectrum depends strongly on the value of  $\epsilon_h$ .

Liquid	Calculations		Experiment	
	Ordered medium	Disordered medium	GATR I (Si window)	GATR II (Al window)
<b>I. <math>CHCl_3</math></b>				
Bulk		756.0	752	753
3D	759.1	758.1		
2D	760.1	759.8		759.2
1D	771.1	771	772	
P=1/3	761.1	673.2		
P=3	756.9	659.5		
<b>II. <math>C_6H_6</math></b>				
Bulk		672.7	671	671
3D	673.3	673.3		
2D	673.8	673.6		675
1D	678.6	678.4	678.6	
P=1/3	674.4	673.8		
P=3	672.8	673.4		
<b>III. <math>CS_2</math></b>				
Bulk		1502.7	1501	1500
3D	1505.4	1505.4		
2D	1507.5	1506.7		1513
1D	1527.7	1527.2	1531	
P=1/3	1509.7	1507.4		
P=3	1503.4	1506.0		

Table 1. Calculated and experimental peak positions,  $\nu$  ( $cm^{-1}$ ), of the most intense IR absorption band observed for liquid  $CHCl_3$ ,  $C_6H_6$  and  $CS_2$  under various dielectric confinement conditions ( $\epsilon_h=13.6$ , Si/Ge)

Host Matrix, $\epsilon_h$	Bulk benzene, $\nu_{bulk}$	Ordered			Disordered		
		1D	2D	3D	1D	2D	3D
2.2		681.4 (0.42)	677.3 (0.41)	675.7 (0.42)	673 (0.34) 681 (2.2)	676.2 (0.36)	675.7 (0.42)
5	672.7 (4.56)	680.4 (1.69)	675.3 (0.76)	674.3 (0.63)	680 (0.65) 673 (1.4)	674.8 (0.63)	674.2 (0.63)
11.56		678.9 (5.63)	674 (1.09)	673.5 (0.78)	678.8 (1.99)	673.8 (0.87)	673.5 (0.78)
16		678.2 (8.26)	673.7 (1.19)	673.3 (0.82)	678.1 (2.19)	673.6 (0.94)	673.3 (0.82)

Table 2. Peak position (in  $cm^{-1}$ ) and intensity (in brackets) for dielectric loss spectra of two component composite medium consisting of ordered and disordered benzene mesoparticles under 1D, 2D and 3D dielectric confinement in various host matrices ( $f=0.1$ )

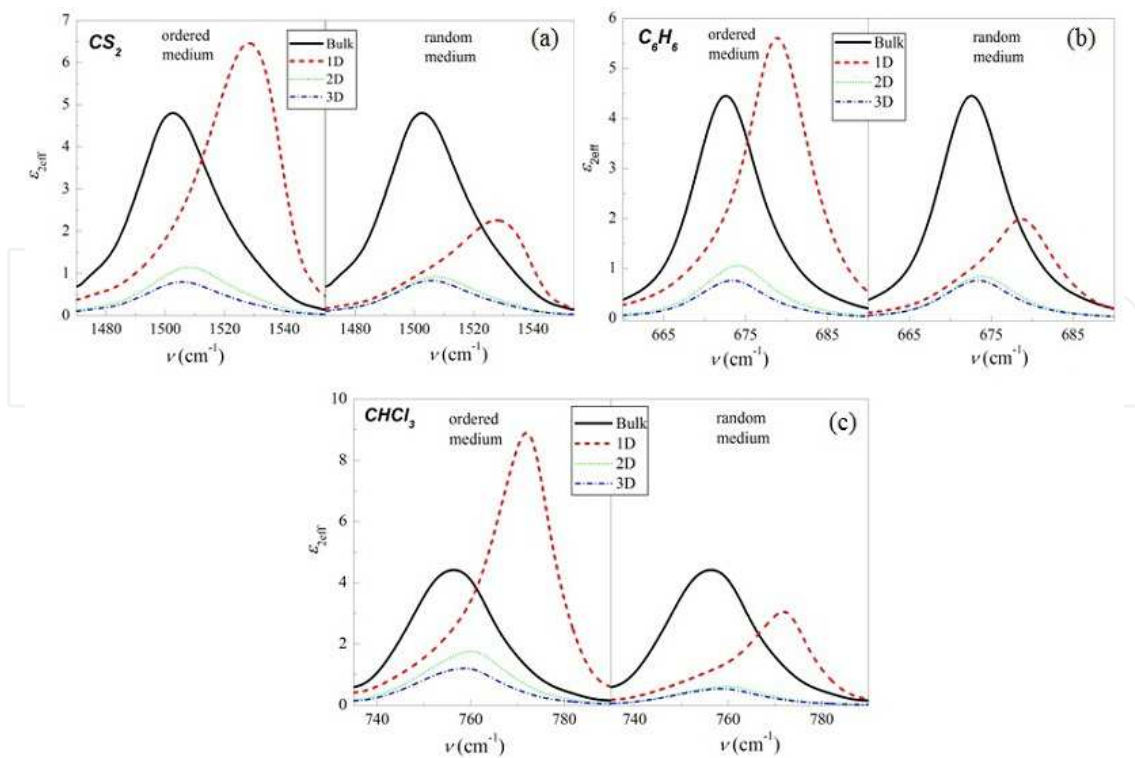


Fig. 3. Calculated dielectric loss spectra  $\epsilon_{2\text{eff}}(\nu)$  of liquids (a)  $\text{CS}_2$ , (b)  $\text{C}_6\text{H}_6$  and (c)  $\text{CHCl}_3$  under the conditions of different size confinement for ordered and disordered (random) media. The calculations were performed using equations (8) and (15a) at  $f=0.1$ ,  $\epsilon_h=11.56$

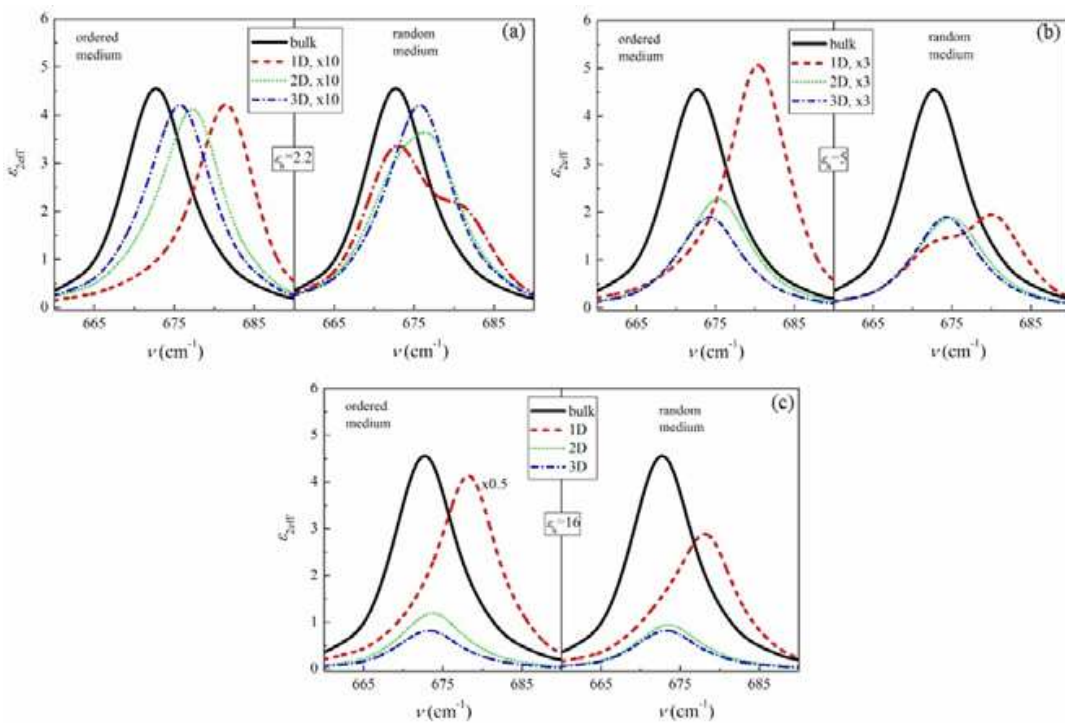


Fig. 4. Dielectric loss spectra of benzene mesoparticles calculated for ordered and random composite media at different confinement conditions for various matrixes (a)  $\epsilon_h=2.2$  glass, (b)  $\epsilon_h=5$ , (c)  $\epsilon_h=11.56$  silicon, and (d)  $\epsilon_h=16$  germanium

Calculations of the dielectric loss spectra of mesoparticles of amorphous  $\text{SiO}_2$  under various types of dielectric confinement are presented in Fig. 5 and summarised in Table 3. The calculations were performed at  $f = 0.2$  and  $\epsilon_h = 2.34$  for KBr. The optical properties of amorphous  $\text{SiO}_2$  were obtained from Ref. (Efimov, 1995). Amorphous  $\text{SiO}_2$  has several absorption bands, with peaks at  $468 \text{ cm}^{-1}$  (Si-O-Si rocking vibrational mode),  $808 \text{ cm}^{-1}$  (O-Si-O bending mode) and  $1082 \text{ cm}^{-1}$  (Si-O asymmetric stretching mode). In our analysis, we focus mainly on the most intense band at  $1082 \text{ cm}^{-1}$ .

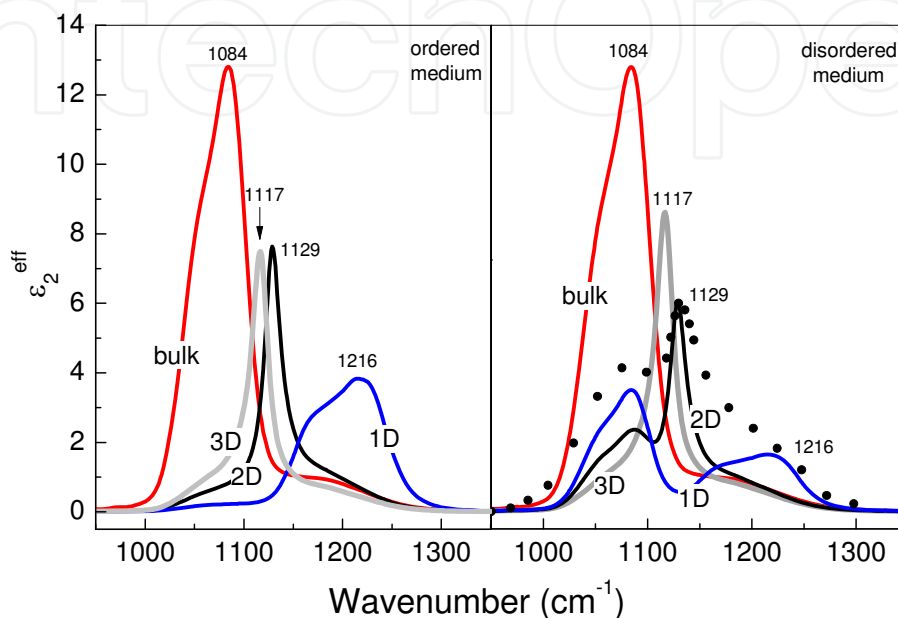


Fig. 5. Calculated dielectric loss spectra of bulk  $\text{SiO}_2$  and its composites under dielectric confinement in a host medium with  $\epsilon_h=2.34$  (KBr) and filling factor  $f=0.2$  for ordered (left panel) and disordered (right panel) mesoparticles. The circles on the right panel correspond to experimental data for  $\text{SiO}_2/\text{Si}$  rods in a KBr matrix from Noda et al., 2005

The principal features of the calculated spectra are shown in Figs. 2 - 5 and the results of our calculations are summarized in Tables 1 - 3. For all the calculated model composites viz. benzene, chloroform, carbon disulphide and  $\text{SiO}_2$ , the position of the dielectric loss spectral maximum, and its intensity, depends on the dielectric permittivity of the host medium. For larger  $\epsilon_h$ , the peak position is shifted to smaller wavenumbers towards the peak of the bulk medium. The peak intensity increases significantly for larger values of  $\epsilon_h$ , for example, by a factor of 2 for  $\text{C}_6\text{H}_6$  in Figs. 2(a) and 4(c), for  $\text{CHCl}_3$  in Fig. 3c and for  $\text{CS}_2$  in Fig. 2(b). In all cases, the maximal spectral shift of the dielectric loss spectrum is observed under 1D dielectric confinement. The peak positions for 2D and 3D confinement are closer to the peak position observed from bulk benzene and carbon disulphide. The difference in peak position for 2D and 3D confinement is very small and is more apparent for small  $\epsilon_h$ . For benzene mesoparticles embedded in the host matrix, with  $\epsilon_h = 2.2$  or  $\epsilon_h = 5$ , the appearance of the second peak is clearly seen under 1D confinement in disordered media (see Fig. 4 (a and b) and Table 2). Similar results are also apparent in Fig. 2(d) for  $\text{CS}_2$  at  $\epsilon_h = 3$ . Note that at smaller  $\epsilon_h$ , the peak related to the bulk mode is more intense, while for larger  $\epsilon_h$ , the peak corresponding to 1D confinement has a higher intensity. For both  $\text{C}_6\text{H}_6$  and  $\text{CS}_2$ , the peak related to the bulk mode significantly reduces in intensity, indeed, it practically disappears at  $\epsilon_h = 13.6$  as seen in Fig. 2 (a and b). It is also worth noting that the peak intensity of the

dielectric loss spectrum for an ordered composite medium at  $f = 0.1$  and  $\epsilon_h = 16$ , in a germanium host matrix, is approximately two times higher than that for bulk benzene (Table 2), while it is 10 times lower at  $\epsilon_h = 2.2$ .

Sample	Dielectric matrix	Bulk, peak position	Calculations, DLF method, peak position, (cm <sup>-1</sup> )			Experiment, peak position, (cm <sup>-1</sup> )		
	$\epsilon_h$	$\nu_{\text{bulk}}$ , cm <sup>-1</sup>	$\nu_{3D}$	$\nu_{2D}$	$\nu_{1D}$	$\nu_{3D}$	$\nu_{2D}$	$\nu_{1D}$
SiO <sub>2</sub>	1, air		1143	1164	1252			1257 <sup>d</sup>
					1253 <sup>a</sup>			1253 <sup>e</sup>
					1250 <sup>b</sup>			
	2.34, KBr	1084	1117	1129	1216		1130 <sup>c</sup>	
						1109		
	1.77, water		1109	1118	1142			

<sup>a</sup>From transmission spectra calculated at 65° of incident light using TMM; <sup>b</sup>from minimum of the reflection spectrum calculated for *p*-polarized light at incidence angle of 70° using expressions of multilayer stack optics; <sup>c</sup>experimental data from Noda et al., 2005; <sup>d</sup>experimental data from Shaganov et al., 2001; <sup>e</sup>experimental data from Röseler, 2005.

Table 3. Experimental and calculated peak positions,  $\nu$  (cm<sup>-1</sup>), of IR absorption bands observed for SiO<sub>2</sub> under various dielectric confinement conditions

### 3.2 Experimental

Infrared absorption spectra were measured on an FTS 6000 Fourier Transform Infrared (FTIR) spectrometer using a commercially available Grazing angle Attenuated Total Reflection (ATR), attachment from the Harrick Scientific Corporation. Absorption measurements were made on both thick and thin layers of liquid, as well as on thin solid films. For measurements of absorption for the bulk, thick layer, a drop of liquid approximately 1 mm thick was placed in the middle of the Ge ATR element. In order to achieve dielectric confinement in the liquids studied, three methods were used. In the first technique, absorption spectra were measured using the Grazing angle Attenuated Total Reflection (GATR) attachment. A thin film of liquid was obtained by confining the liquid between the Ge ATR prism and the 4 mm thick silicon top window, see Fig. 6(a). In the second method, an Al coated glass substrate was used instead of the Si top window Fig. 6(b). The strength of window compression was changed using the GATR pressure applicator control. Measurements were performed in *p*-polarized light at a 60° angle of incidence. The third method for exploring dielectric confinement effects is based on the use of a macro-porous silicon matrix, with liquid infiltrated into the pores (Perova et al., 2009). In our study, porous Si samples were fabricated by electrochemical etching of single-crystalline (100) *n*-type Si wafers in a HF (48%) : H<sub>2</sub>O = 2:3 solution. Etching was performed for 30 mins at a current density of 16 mA/cm<sup>2</sup>. The resulting pore diameter was about 0.8 μm. All three liquids studied evaporated completely from the pores approximately 30-40 minutes after infiltration. Therefore, in-situ FTIR measurements were carried out immediately after liquid infiltration using a registration time of ~ 20 sec and a dwell time of ~ 5 sec.

All the liquids investigated were of high purity, purchased from Sigma-Aldrich. The Ge ATR prism and Si windows were new and of excellent optical quality. The Ge ATR element was carefully cleaned before the drop of liquid was placed on it. The glass substrate with the

Al layer was freshly prepared; a new element was used for each experiment. At least five separate experiments were performed for each liquid. These precautions enabled us to avoid the influence of any unwanted interactions.

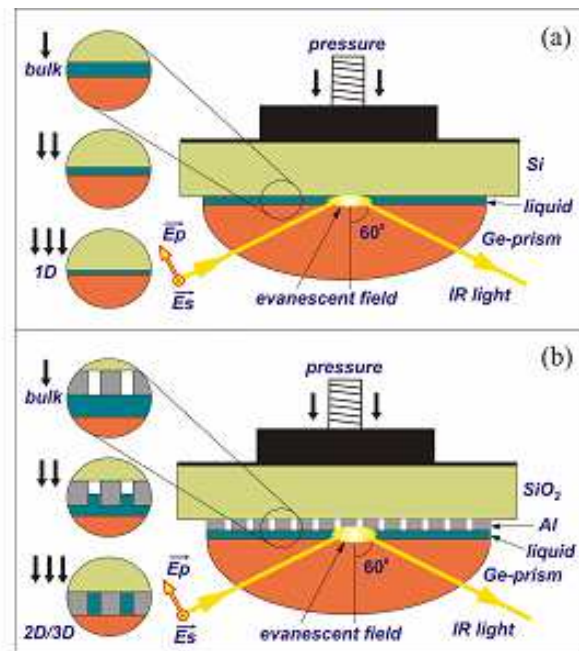


Fig. 6. Schematic of FTIR experiments using GATR attachment for (a) Si and (b) Al top window

Thin films of  $\text{SiO}_2$  were deposited onto an Al coated glass substrate using an electron-gun evaporator. In order to register the LO-phonons, or the absorption spectrum of these materials under 1D confinement, we used an oblique incidence of light in *p*- and *s*-polarisations, using the Reflection-Absorption (RA) and GATR attachments, see Ref. (Shaganov et al., 2003) for details. For registration of spectra under 3D confinement, we used  $\text{SiO}_2$  spherical particles of different diameters dissolved in water. Spherical particles of  $\text{SiO}_2$ , with a diameter of 193 nm, coated with an ultra-thin layer of surfactant to prevent particle conglomeration and dissolved in water, were purchased from Sigma-Aldrich. The distribution of particles size in the solution is  $\pm 5 - 10$  nm, as guaranteed by the manufacturer.

### 3.3 Comparison of experimental and calculated data

#### a) Liquid systems

Absorption spectra obtained for three of the liquids under investigation are shown in Figs. 7(a) - 7(c). From Fig. 7(a), it is apparent that, for a thick chloroform layer, an absorption band with a peak position at  $\nu = 752 \text{ cm}^{-1}$ , corresponding to the bulk mode, is observed. At the maximum possible confinement, when the layer is only  $\sim 100\text{-}200$  nm thick, the absorption peak shifts to  $\nu = 771 \text{ cm}^{-1}$ . This value agrees very well with calculations of the dielectric loss spectrum of liquid  $\text{CHCl}_3$  under 1D dielectric confinement (see Table 1). We believe that the line width increase observed for the absorption band at  $760 \text{ cm}^{-1}$  is due to the fact that the absorption band for this intermediate case is a superposition of the absorption bands obtained in the presence and absence of the dielectric confinement effect. We would like to emphasise that the position and shape of the weaker absorption band, observed for  $\text{CHCl}_3$  at  $\nu = 1215 \text{ cm}^{-1}$ , remained unchanged as expected (see Fig. 7(a)).

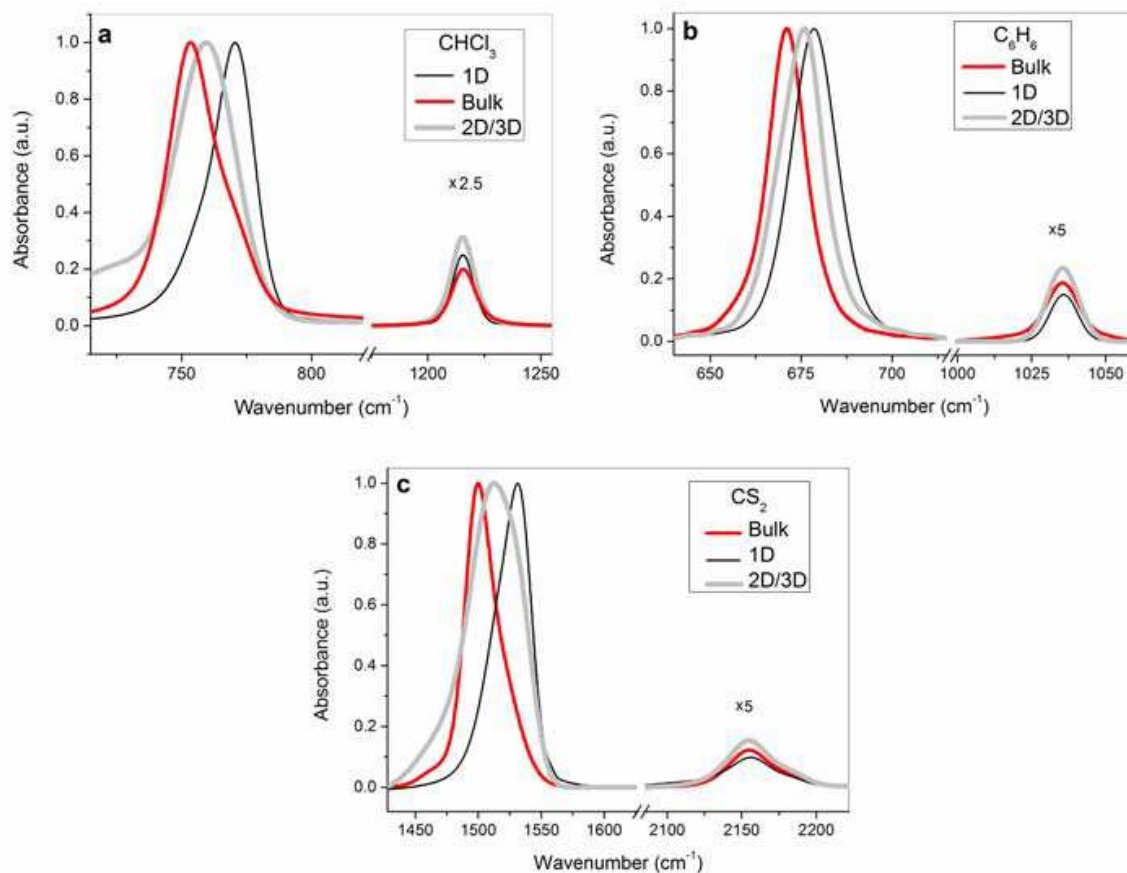


Fig. 7. Normalized infrared spectra of liquids (a)  $\text{CHCl}_3$ , (b)  $\text{C}_6\text{H}_6$  and (c)  $\text{CS}_2$  registered with GATR attachment. Note that the absorbance of the vibrational bands with small intensities was multiplied by slightly different factors, shown beside the bands, to demonstrate clearly that they have the same peak position

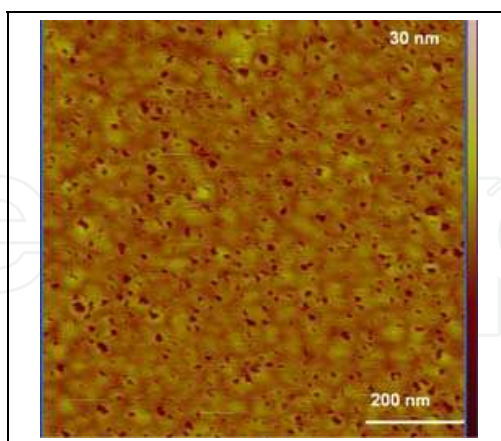


Fig. 8. Top view AFM image of the Al coated glass substrate

Similar behaviour was observed for liquid benzene (Fig. 7(b)), where the frequency of the spectral maximum for the bulk liquid, initially observed at  $\nu = 671 \text{ cm}^{-1}$ , was shifted under strong confinement to  $\nu = 679 \text{ cm}^{-1}$ , corresponding to 1D dielectric confinement of a very thin layer of  $\text{C}_6\text{H}_6$ . The same effect was observed in liquid  $\text{CS}_2$  (Fig. 7(c)) with a frequency shift from  $\nu = 1501 \text{ cm}^{-1}$ , observed for the bulk material, to  $\nu = 1532 \text{ cm}^{-1}$ , measured under 1D

confinement. As in the case of chloroform, the layer thickness for the benzene and carbon disulphide was estimated to be 100 - 200 nm. The position and shape of the weak absorption band observed at  $1036\text{ cm}^{-1}$  for  $\text{C}_6\text{H}_6$ , and at  $2155\text{ cm}^{-1}$  for  $\text{CS}_2$ , remain unchanged (see Figs. 7(b) and 7(c)). We also note that the largest peak shift due to dielectric confinement was observed for  $\text{CS}_2$  with the largest integrated intensity of infrared absorption band of all the liquids investigated.

In order to measure the vibrational spectra of these liquids under 2D/3D dielectric confinement, we modified the experimental setup as follows (see Fig. 6(b)). The top silicon window was replaced with a 5 mm thick glass plate, coated with a thin,  $\sim 0.1\ \mu\text{m}$ , Al layer. The coating was applied by evaporation of Al wire in a bell jar evaporator. Under these evaporation conditions, the Al film contains pores, with diameters ranging from a few microns to tens of nanometers. A small drop of liquid was placed on top of the ATR Ge prism, then the Al coated glass plate was placed on top and the experiment was immediately run as the level of compression of the top glass window was increased. The effects of confinement on the liquid spectra were practically identical to those described earlier, with the exception of the last stage. When the thin layer of liquid evaporated completely, the maximum frequency in the spectrum shifted to  $\sim 760\text{ cm}^{-1}$  for  $\text{CHCl}_3$ ,  $676\text{ cm}^{-1}$  for  $\text{C}_6\text{H}_6$  and to  $1513\text{ cm}^{-1}$  for  $\text{CS}_2$  (see Fig. 7 and Table 1). These frequencies are in good agreement with data calculated for 2D or 3D dielectric confinement. This can be seen in Table 1 and from Figs. 2, 3 and 7. Note that the infiltration of the liquid into the voids, or pores, in the Al layer was confirmed by the fact that the spectra related to 2D/3D confinement were still observed several hours after initial sample preparation, when the thin layer of liquid between the Ge prism and the Al coated substrate had definitely evaporated. As the deposited layer of Al is too thin to consider the "porous" Al layer obtained as a matrix for the fabrication of liquid wires, the diameter/length ratio of the pores obtained suggests that we are dealing with liquid spheres embedded in a porous Al matrix situated at the top of the Ge prism. The results of surface analysis of the Al coated glass substrate using an Atomic-Force Microscope (AFM) confirms the existence of the void structure (with width and depth of voids at around  $\sim 20\text{-}40\text{ nm}$  and  $\sim 10\text{-}15\text{ nm}$ , accordingly) of the substrates used for these experiments (see Fig. 8). From Table 1, the peak positions observed under 2D and 3D confinement are close, making it difficult to draw firm conclusions. Nevertheless, we believe that with this experiment, it is possible to obtain information on the absorbance spectra of the liquids investigated under 3D confinement.

Fig. 9 shows the behaviour of the absorption spectra of benzene infiltrated into a macroporous silicon matrix registered at various times after infiltration. The position of the absorption band for benzene immediately after infiltration was close to the frequency of the bulk mode of  $\text{C}_6\text{H}_6$  ( $\nu = 673\text{ cm}^{-1}$ ). During the course of evaporation, the peak position shifted to higher frequencies and  $\nu = 682\text{ cm}^{-1}$  at the end of the registration process. We believe that at the beginning of the registration process, the pores were totally filled with liquid benzene. Since the pore diameter is larger than that necessary to satisfy the criteria for dielectric confinement, the absorption spectrum observed is that from the bulk liquid. In the course of drying out, the liquid bulk phase of the  $\text{C}_6\text{H}_6$  evaporates, leaving a thin layer of adsorbed liquid on the pore surface. When the electric field of the incident light is oriented parallel to the sample surface, the conditions for the registration of 1D dielectric confinement are met, as shown in the insert in Fig. 9. These results are in good agreement with our calculations shown in Fig. 3(b). Similar results were obtained for  $\text{CHCl}_3$  and for  $\text{CS}_2$ , these results are summarized in Table 1. It should be noted that, due to the faster

evaporation of  $\text{CHCl}_3$  and the  $\text{CS}_2$  liquids from the pores, it was not possible to register the bulk mode at the beginning of the registration process. In conclusion, we note that since exact values of layer thickness and the sphere diameter distribution were not known, we were unable to calculate the imaginary part of the dielectric function from the experiment, in order to compare this with the calculated values  $\varepsilon_2^{\text{eff}}(\nu)$ . Therefore, the position of the absorbance spectra,  $A(\nu)$ , was used for this comparison. However, it is well known that for strong and narrow isolated absorption bands, the peak positions of  $\varepsilon_2(\nu)$  and  $A(\nu)$  are close to each other. Our estimates have shown that, in this case, the deviation does not exceed 1 - 2  $\text{cm}^{-1}$ .

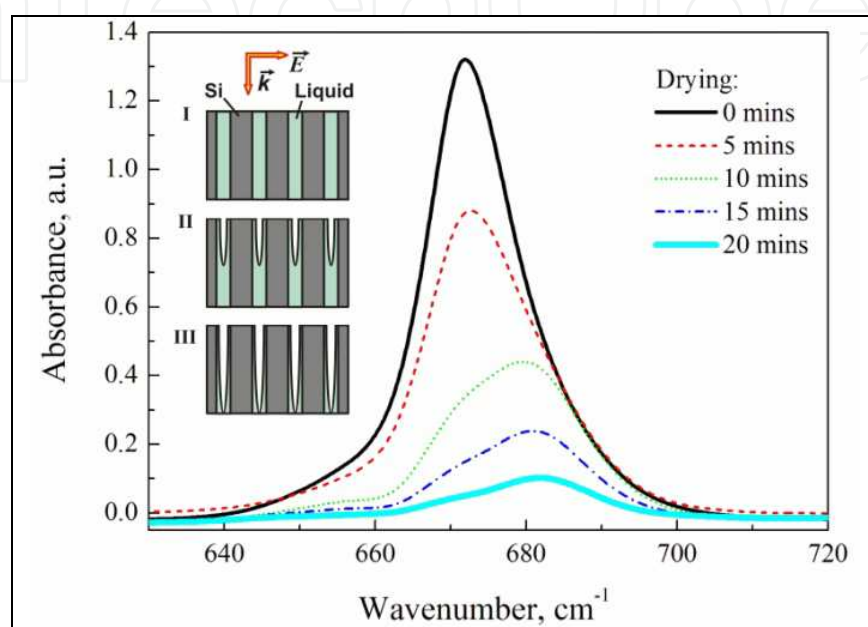


Fig. 9. Absorbance spectra of benzene infiltrated into silicon pores. Insert: Schematic diagram of the conversion of liquid infiltrated into the macro-porous silicon matrix from a bulk liquid phase to a liquid under 1D dielectric confinement as a result of the drying process.

Reproduced with permission of journal Chemical Physics Letters (Perova et al., 2009)

### (b) Amorphous solids ( $\text{SiO}_2$ )

Calculations of the dielectric loss spectra of mesoparticles of amorphous  $\text{SiO}_2$  under various types of dielectric confinement are presented in Fig. 4 and summarised in Table 3. The peak position for 1D dielectric confinement is confirmed experimentally in our earlier paper (Shaganov et al., 2003) for 70 nm thick thermally grown oxide, as well as by a number of other papers where the IR spectra of thin (Shaganov et al., 2001; Almeida, 1992; Olsen & Schimura, 1989) and ultra-thin (with a thickness of 5nm) (Tolstoy et al., 2003) films of amorphous  $\text{SiO}_2$  were measured under oblique incidence of IR light. It is worth noting that the shift in the peak position of the Si-O-Si band at  $\sim 1100 \text{ cm}^{-1}$  to higher frequencies ( $\sim 1253 \text{ cm}^{-1}$ ) was also observed in an  $\text{SiO}_2$  thin film under oblique incidence of light using infrared spectroscopic ellipsometry (see Ref. (Röseler, 2005) for details).

In order to lend further support to the model suggested, we performed calculations of the transmission spectra for  $\text{SiO}_2$  thin films under oblique incidence of light, corresponding to 1D confinement, using a  $2 \times 2$  Transfer Matrix Method (TMM) (Azzam & Bashara, 1977). The peak positions of the transmission spectra obtained are included in Table 3. In addition, the peak position of the transmission spectra for thin  $\text{SiO}_2$  films, calculated at oblique incidence of light, is also shown in Table 3. These calculations are performed using expressions from

paper (Shaganov et al., 2001). The results obtained for 1D confinement in an  $\text{SiO}_2$  thin film demonstrate very good agreement between the theory developed for the calculation of the optical properties of a multilayer stack and the approach suggested in this paper. These results are also in agreement with both spectroscopic ellipsometry and infrared spectroscopy experiments at oblique incidences of light.

The spectra calculated for the disordered composite, for 2D confinement, are confirmed experimentally using results published recently in Ref. (Noda et al., 2005), where the infrared spectra of  $\text{SiO}_2/\text{Si}$  disordered nanowires embedded in KBr pellets were investigated. We believe that the peak observed in paper (Noda et al., 2005) at  $\sim 1130 \text{ cm}^{-1}$  and assigned by the authors to a highly disordered structure of thin  $\text{SiO}_2/\text{Si}$  nanowires can be reinterpreted, in the light of the results presented in this paper, as being due to 2D dielectric confinement of amorphous  $\text{SiO}_2$ .

Finally, the infrared spectra of spherical  $\text{SiO}_2$  particles in an aqueous solution have been measured using a GATR attachment. Spherical particles, with diameters of 193 nm, coated with an ultra-thin layer of surfactant to prevent particle conglomeration and dissolved in water, were supplied by Sigma-Aldrich. As noted earlier, the particle size distribution guaranteed by the manufacturer is  $\pm 5 - 10 \text{ nm}$ . The solution was shaken intensely before placing a drop of the liquid onto the Ge ATR prism. The infrared spectra of the  $\text{SiO}_2$  mesoparticles obtained in this experiment are shown for spherical particles of diameter 193 nm in Fig. 10, along with calculations for 3D confinement at  $\epsilon_h = 1.77$ . Good agreement between the experimental and calculated spectra can be seen for this composite. The minor discrepancies between the experimental and calculated spectra of the spherical  $\text{SiO}_2$  particles observed in the spectrum wing regions is due to the fact that silicon dioxide can exist in various forms such as amorphous quartz, fused quartz or quartz doped with impurities. The exact structure of the Sigma-Aldrich silicon dioxide spherical particles is not known. For our calculations, the optical constants of amorphous quartz were taken from the literature, which can result in differences between the calculated spectra from the experimental data in the wing regions.

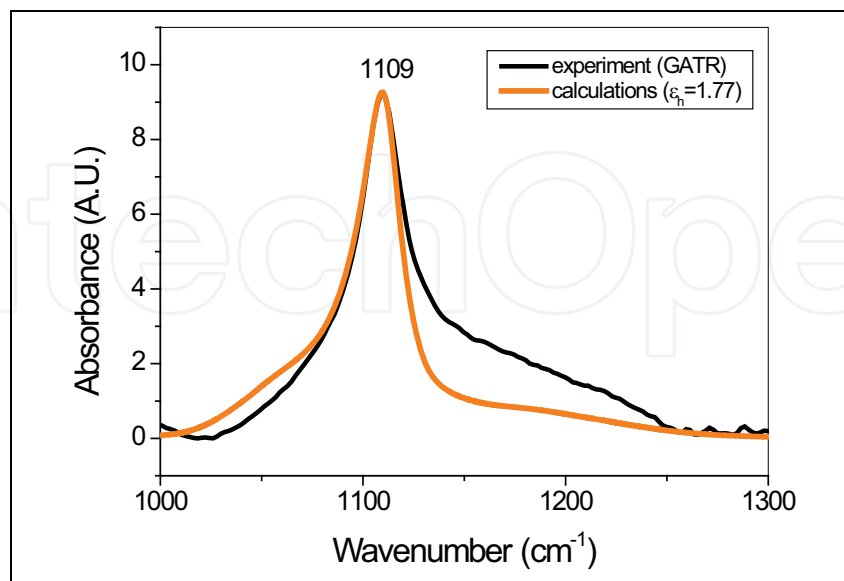


Fig. 10. Absorbance spectra of  $\text{SiO}_2$  spherical particles (thin line) diluted in water with a diameter of 193 nm shown together with the calculated spectra (thick line) based on Eqn. (15a) at  $\epsilon_h = 1.77$

#### 4. Conclusions

The experimental results presented here demonstrate good agreement with calculations made using the model suggested for estimating the effect of 1D, 2D and 3D dielectric confinement on the IR spectra of condensed matter. The results obtained allow us to conclude that the physical mechanism responsible for the shift of the absorption peak of small particles experiencing different types of dielectric confinement is the same, regardless of the nature of the condensed medium, whether crystalline or amorphous, solid or liquid. The shift is due to the local field effect acting on the size confined particles, surrounded by the dielectric matrix.

The expression obtained for particle absorption under 1D confinement is the same as that for the dielectric loss spectrum of the crystal at the frequency of the longitudinal-optical phonons (Berreman, 1963). This indicates that similar absorption bands to those seen under 1D confinement will be observed near the minimum of the real part of the dielectric function ( $\text{Re}\epsilon(\nu)$ ) function in any condensed medium. This has been confirmed already in other studies on thin films of amorphous solids (Payne & Inkson, 1984; Röseler, 2005; Tolstoy et al., 2003; Röseler, 2005; Shaganov et al., 2005), polymer monolayers (see (Yamamoto & Masui, 1996) and references therein) as well as for the thin liquid films investigated in this work. We conclude that the absorption bands, observed earlier and ascribed to the Berreman effect (Berreman, 1963), are a particular case of the manifestation of 1D confinement. This conclusion is supported by a study by (Lehmann, 1988), where it was shown that the appearance of the absorption band at the frequency of the LO-phonons in an amorphous dielectric is a consequence of the boundary conditions in a dielectric film at an oblique incidence of the probe beam.

The numerical and experimental results described above indicate that relatively large spectral effects can be expected as a result of dielectric confinement. Our results convincingly demonstrate that the blue shift of the absorption bands under dielectric confinement can be significant, and must be taken into account when interpreting experimental spectroscopic data from composite systems. Of course, we ignored the resonance dipole-dipole interactions, which are negligible at particle volume concentrations of less than 1% and will not impact the accuracy of the calculations for filling factors of less than 10%.

We note that the expressions obtained only deal with isolated particles of spheroidal shape and are valid when the spheroidal semi-axes in either one, two or three directions are satisfied by the conditions  $d_z \ll \lambda$  or  $d_x = d_z \ll \lambda$  while remaining larger than atomic dimensions. Therefore, the approach suggested here can be used for a general description of the spectral characteristics of arbitrary micro-objects, or more specifically, sub-micron microcrystalline particles, under dielectric confinement. One of the disadvantages of our approach is the absence of the size parameter in the model. Obviously, the response of the dielectric medium will change with a decrease in the particle size, approaching frequencies characteristic of the limited cases of 1D, 2D and 3D confinement considered in this work. There is evidence to indicate that this assumption is justified, assuming the optical properties are linear. We believe that particle size will play a significant role only when quantum confinement effects influences their non-linear optical properties. Other physical phenomena need to be taken into account in order to calculate the absolute value of the imaginary part of dielectric function. These phenomena include sample surface roughness, polaritons, diffraction and scattering. In addition, the specificity of the molecular orientation in, for example, Langmuir-Blodgett films, or the film structure, that is, anisotropy, of the oxide or island-like surface structure for ultra-thin films, or monolayers, may also influence

the shape and position of the IR spectra. Therefore, further development of this theory and its experimental verification is required.

We conclude that dielectric confinement offers considerable promise as a method for tuning the absorption properties of composite media. The approach allows control of both the position and intensity of the dielectric loss spectrum of the absorbing medium embedded in a composite. Furthermore, the absorption efficiency can be increased significantly due to local field effects. Clearly, further development of simple models for the description of the spectral properties of composite media, including meso-composites based on porous semiconductors, as well as other porous media with absorbent inclusions, is still necessary. The most important applications of these studies are to the analysis of the absorption spectra of industrial smokes, toxic aerosols and liquid droplets, (see Ref. (Carlton et al., 1977; Carlton, 1980) for example) as well as for colloidal optofluidic systems (Psaltis, 2006).

## 5. Acknowledgments

The authors would like to acknowledge V. Melnikov, S. Dyakov and Alex Gunko for help with the experiments and calculations. V. Tolmachev is acknowledged for useful discussions.

## 6. References

- Aspnes, D.E. (1982). Local field effects and effective-medium theory: A macroscopic perspective. *Amer.J.Phys.*, 50, 8, 704-708, ISSN: 00029505.
- Almeida, R.M. (1992). Detection of LO modes in glass by infrared reflection spectroscopy at oblique incidence, *Phys. Rev. B*, 45, 1, 161-170, 1 January. ISSN: 1098-0121.
- Azzam, R.M.A. & Bashara, N.M. (1997). *Ellipsometry and polarized light*, Elsevier B.V., ISBN: 0-444-87016-4, Amsterdam, The Netherlands.
- Bakhshiev, N. G.; Girin, O. P. & Libov, V. S. (1962). The relationship between the measured and intrinsic absorption spectra in condensed medium.I. *Sov.Phys.Dokl.* 145, 3, 1025-1027.
- Bakhshiev, N. G.; Girin, O. P. & Libov, V. S. (1963). The relationship between the measured and intrinsic absorption spectra in condensed medium.II. *Sov. Opt. & Spectr.* 1963, 14, 745-750 (English. Translation: *Opt.Spectry.* 14, 2, 395-400).
- Barnes, D. W. & Schatz, P. N. (1963). Optical Constants and Absolute Intensities from Infrared Reflection Measurements. The 6.6- $\mu$  Band of Liquid CS<sub>2</sub> and 13- $\mu$  Doublet of liquid CCL<sub>4</sub>. *J. Chem. Phys.*, 38, 11, 2662-2667, ISSN: 0021-9606.
- Berreman, D.W. (1963). Infrared Absorption at Longitudinal Optic Frequency in Cubic Crystal Films, *Phys. Rev.*, 130, 6, 2193-2198, 15 June.
- Bruggeman, D.A.G. (1935). Berechnung verschiedener physikalischer Konstanten von heterogenen Substanzen, *Ann. Phys. (Leipzig)* 24, 636-679.
- Böttcher C.I.F. (1952). *Theory of Electric Polarisation*, Elsevier, Amsterdam.
- Cahay, M.; Leburton, J.-P.; Lockwood, D.J.; Bandyopadhyay, S. & Harris, J.S. (2001). *Quantum Confinement VI: Nanostructured materials and Devices*, Electrochemical Society, Inc., ISBN: 1-56677-352-0, New Jersey, USA.
- Cao, G. (2004). *Nanostructures and Nanomaterials: Synthesis, Properties and Applications*, Imperial College Press, ISBN: 1-86094-415-9, London, UK.
- Carlton, H. R.; Anderson, D. H.; Milham, M. E.; Tarnove, T. L.; Frickel, R. H. & Sindoni, I. (1977). Infrared extinction spectra of some common liquid aerosols, *Appl. Opt.*, 16, 6, 1598-1605, ISSN: 1559-128X.

- Carlson, H. R. (1980). Aerosol spectrometry in the infrared, *Appl. Opt.*, 19, 13, 2210-2218. ISSN: 1559-128X
- Chemla, D. S. & Miller, D.A.B. (1986). Mechanism for enhanced optical nonlinearities and bistability by combined dielectric–electronic confinement in semiconductor microcrystallites, *Opt. Letters*, 11, 8, 522-524, ISSN: 0146-9592.
- Clifford, A. A. & Crawford, B. (1966). Vibrational Intensities. XIV. The Relation of Optical Constants to Molecular Parameters. *J. Phys. Chem.*, 70, 5, 1536-1543.
- Cohen, R.W.; Cody, G. D.; Coutts, M. D. & Abeles, B. (1973). Optical Properties of Granular Silver and Gold Films. *Phys. Rev. B*, 8, 8, 3689-3701, ISSN: 1098-0121.
- DeLeeuw, S. W. & Thorpe, M. F. (1985). Coulomb splittings in glasses. *Phys. Rev. Lett.*, 55, 26, 2879-2882, ISSN: 0031-9007.
- Dolgaleva, K.; Boyd, R.W. & Millionni, P.W. (2009). The effects of local fields on laser gain for layered and Maxwell Garnett composite materials. *J. Opt. A: Pure Appl. Opt.*, 11, 2, ISSN:14644258.
- Efimov, A.M. (1995). *Optical Constants of Inorganic Glasses*, CRC Press, Inc., ISBN: 0-8493-3783-6, New York, USA.
- Foss, C.A.; Hornyak, G.I., Stockert, J.A. & Martin C.R. (1994). Template-Synthesized Nanoscopic Gold Particles: Optical Spectra and the Effects of Particle Size and Shape. *J. Phys. Chem. B*, 98, 11, 2963-2971, ISSN: 1520-6106.
- Fröhlich, H. (1949). *Theory of Dielectrics*, Clarendon Press, Oxford.
- Ghiner, A.V. & Surdutovich, G. I. (1994). Method of integral equations and an extinction theorem for two-dimensional problems in nonlinear optics. *Phys. Rev. A*, 50, 1, 714-723, ISSN: 1050-2947; (1994). Beyond the Lorentz-Lorenz Formula. *Optics & Photonics News*, 5, 12, December, 34-35, ISSN: 10476938.
- Golovan, L. A.; Kuznetsova, L. P.; Fedotov, A. B.; Konorov, S. O.; Sidorov-Biryukov, D. A.; Timoshenko, V. Yu.; Zheltikov, A. M.; and Kashkarov, P. K. (2003). Nanocrystal-size-sensitive third-harmonic generation in nanostructured silicon. *Appl. Phys. B*, 76, 4, 429-433, ISSN: 0946-2171.
- Golovan, L. A.; Timoshenko, V. Yu. & Kashkarov, P. K. (2007). Optical properties of porous-system-based nanocomposites, *Physics-Uspekhi*, 50, 6, 595-612, ISSN: 1063-7869; Golovan', L.; Kashkarov, P. & Timoshenko, V. (2007). Form birefringence in porous semiconductors and dielectrics: A review. *Crystal. Reports*, 52, 4, 672-685, ISSN: 1063-7745.
- Heitler, W. (1975). *Quantum Theory of Radiation*, 3rd ed., Wiley, ISBN: 0486645584, New York.
- Hornyak, G.L.; Patrissi, C.J. & Martin, Charles R. (1997). Fabrication, Characterization, and Optical Properties of Gold Nanoparticle/Porous Alumina Composites: The Nonscattering Maxwell-Garnett Limit. *J. Phys. Chem B*, 101, 9, 1548-1550, ISSN: 1520-6106.
- Iglesias, J. E.; Ocana, M. & Serma, C.J. (1990). Aggregation and Matrix Effects on the Infrared Spectrum of Microcrystalline Powders. *Appl. Spectr.*, 44, 3, 418, ISSN: 0021-9037.
- Lamberti, C. (2008). *Characterization of Semiconductor Heterostructures and Nanostructures*, Elsevier, ISBN: 0-44453-099-1, Amsterdam, The Netherland; Oxford, UK.
- Lehmann, A. (1988). Theory of Infrared Transmission Spectra of Thin Insulating Films, *Phys. Stat. Sol. B*, 148, 1, 401-405.
- Liu, A. (1994). Local-field effect on the linear optical intersubband absorption in multiple quantum wells, *Phys. Rev. B*, 50, 12, 8569-8576, ISSN: 1098-0121.
- Mallet, P.; Guerin, C. A. & Sentenac, A. (2005). Maxwell-Garnett mixing rule in the presence of multiple scattering: Derivation and accuracy, *Phys. Rev. B*, 72, 1, 14205/1-9, ISSN: 1098-0121.

- Maxwell-Garnett, J.C. (1904). Colours in metal glasses and metal films. *Philos. Trans. R. Soc. London, Sect. A*, Vol. 203, 385-420; (1906). *Philos. Trans. A*, 205, 237-288.
- Noda, T.; Suzuki, H.; Araki, H.; Yang, W.; Ying, S. & Tosa, M. (2005). Microstructures and IR spectra of long amorphous SiO<sub>2</sub>/Si nanowires. *Appl.Sur.Sci.*, 241, 1-2, 231-235. ISSN: 0169-4332.
- Olsen, J.E. & Schimura, F. (1989). Infrared reflection spectroscopy of the SiO<sub>2</sub>-silicon interface. *J. Appl. Phys.*, 66, 3, 1353-1358, ISSN: 0021-8979.
- Osborn, J. A. (1945). Demagnetizing Factors of the General Ellipsoid. *Phys. Rev.*, 67, 11-12, 351-357.
- Palik, D. (1978). *Optical Constants of Solids*, Delta Academic Press, New York, ISBN 0-521-46829-9.
- Perova, T.S.; Shaganov, I. I.; Melnikov, V.A. & Berwick, K. (2009). Direct evidence of the dielectric confinement effect in the infrared spectra of organic liquids, *Chem.Phys.Lett.*, 479, 1-3, 81-85, ISSN: 0009-2614.
- Psaltis, D.; Quake, S.R. & Yang, C. (2006). Developing optofluidic technology through the fusion of microfluidics and optics, *Nature* 442, 7101, 381-386. ISSN: 0028-0836.
- Röseler, A. (2005). Spectroscopic Infrared Ellipsometry. In: *Handbook of Ellipsometry*, H.G. Tompkins, E.I. Irene, (Ed.), 789-797, Springer-Verlag GmbH & Co. KG, ISBN: 3-540-22293-6, Heidelberg, Germany.
- Schmitt-Rink, S., Miller, D. A. B. & Chemla, D. S. (1987). Theory of the linear and nonlinear optical properties of semiconductor microcrystallites. *Phys.Rev. B* 35, 15, 8113-8125, ISSN: 1098-0121.
- Shaganov, I. I.; Perova, T. S.; Moore, R. A. & Berwick, K. (2001). Spectroscopic characteristics of SiO and SiO<sub>2</sub> solid films: Assignment and local field effect influence. *J. Mater. Science: Mater. Electron.*, 12, 4-6, 351-355, ISSN: 09574522.
- Shaganov, I. I.; Perova, T.S.; Moore, R.A. & Berwick, K. (2003). Local field effect on infrared phonon frequencies of thin dielectric films. *Proceed. SPIE*, 4876, 1, 1158-1167, ISSN: 0277-786X.
- Shaganov, I. I.; Perova, T. S.; Moore A. R. & Berwick, K. (2005). Effect of the Internal Field on the IR Absorption Spectra of Small Particles in the Case of 3D, 2D, and 1D Size Confinement. *J. Phys. Chem. B*, 109, 20, 9885-9891, ISSN: 1520-6106.
- Shaganov, I.; Perova, T.; Melnikov, V.; Dyakov, S. & Berwick, K. (2010). The Size Effect on the Infrared Spectra of Condensed Media under Conditions of 1D, 2D and 3D Dielectric Confinement. *J. Phys.Chem. C*, 114, 39, 16071-16081, ISSN: 19327447.
- Spanier, J. E. & Herman, I. P. (2000). Use of hybrid phenomenological and statistical effective-medium theories of dielectric functions to model the infrared reflectance of porous SiC films, *Phys. Rev. B*, 61, 15, 10437-10450, ISSN: 1098-0121.
- Timoshenko, V. Yu.; Osminkina, L. A.; Efimova, A. I.; Golovan, L. A. & Kashkarov, P. K., (2003). Anisotropy of optical absorption in birefringent porous silicon. *Phys. Rev. B*, 67, 11, 113405/1-4, ISSN: 1098-0121.
- Tolstoy, V.P.; Chernyshova, I.V. & Skryshevsky, V.A. (2003). *Handbook of Infrared spectroscopy of ultrathin films*, John Wiley & Sons, Inc., ISBN: 9780471234326, Hoboken, New Jersey.
- Tolstykh, T.S.; Shaganov, I.I. & Libov, V.S. (1974) Spectroscopic properties of optical transitions in the lattice vibration region for ionic crystals, *Sov. Phys. Solid State*, 16, 3, 431-434.
- Ung, T.; Liz-Marzán, L.M. & Mulvaney, P. (2001). Optical Properties of Thin Films of Au@SiO<sub>2</sub> Particles. *J.Phys.Chem B*, 105, 17, 3441-3452, ISSN: 1520-6106.
- Yamamoto K. & Masui A. (1996). TO-LO Splitting in Infrared Spectra of Thin Films. *Appl. Spectr.*, 50, 6, 759-763. ISSN: 0021-9037
- Zolotarev, V. M.; Morozov, V. N. & Smirnova, E. V. (1984). *Optical constants of natural and technical media*, Chemistry, Leningrad.



## **Fourier Transforms - Approach to Scientific Principles**

Edited by Prof. Goran Nikolic

ISBN 978-953-307-231-9

Hard cover, 468 pages

**Publisher** InTech

**Published online** 11, April, 2011

**Published in print edition** April, 2011

This book aims to provide information about Fourier transform to those needing to use infrared spectroscopy, by explaining the fundamental aspects of the Fourier transform, and techniques for analyzing infrared data obtained for a wide number of materials. It summarizes the theory, instrumentation, methodology, techniques and application of FTIR spectroscopy, and improves the performance and quality of FTIR spectrophotometers.

### **How to reference**

In order to correctly reference this scholarly work, feel free to copy and paste the following:

T.S. Perova, I.I. Shaganov and K. Berwick (2011). The Effect of Local Field Dispersion on the Spectral Characteristics of Nanosized Particles and their Composites, Fourier Transforms - Approach to Scientific Principles, Prof. Goran Nikolic (Ed.), ISBN: 978-953-307-231-9, InTech, Available from:  
<http://www.intechopen.com/books/fourier-transforms-approach-to-scientific-principles/the-effect-of-local-field-dispersion-on-the-spectral-characteristics-of-nanosized-particles-and-thei>

**INTECH**  
open science | open minds

### **InTech Europe**

University Campus STeP Ri  
Slavka Krautzeka 83/A  
51000 Rijeka, Croatia  
Phone: +385 (51) 770 447  
Fax: +385 (51) 686 166  
[www.intechopen.com](http://www.intechopen.com)

### **InTech China**

Unit 405, Office Block, Hotel Equatorial Shanghai  
No.65, Yan An Road (West), Shanghai, 200040, China  
中国上海市延安西路65号上海国际贵都大饭店办公楼405单元  
Phone: +86-21-62489820  
Fax: +86-21-62489821

© 2011 The Author(s). Licensee IntechOpen. This chapter is distributed under the terms of the [Creative Commons Attribution-NonCommercial-ShareAlike-3.0 License](#), which permits use, distribution and reproduction for non-commercial purposes, provided the original is properly cited and derivative works building on this content are distributed under the same license.

IntechOpen

IntechOpen